

Received April 5, 2020, accepted May 11, 2020, date of publication May 19, 2020, date of current version June 1, 2020.

Digital Object Identifier 10.1109/ACCESS.2020.2995261

# The Performance Analysis of Downlink NOMA in LEO Satellite Communication System

ZHIXIANG GAO<sup>1</sup>, AIJUN LIU<sup>1</sup>, (Member, IEEE), AND XIAOHU LIANG<sup>1</sup>

College of Communications Engineering, Army Engineering University of PLA, Nanjing 210007, China

Corresponding author: Aijun Liu (liuj.cn@163.com)

This work was supported in part by the National Natural Science Foundation of China under Grant 61671476 and Grant 61901516, in part by the China Postdoctoral Science Foundation under Grant 2019M651648, and in part by the Natural Science Foundation of Jiangsu Province of China under Grant BK20180578.

**ABSTRACT** Non-orthogonal multiple access (NOMA) has the potential to provide higher throughput than conventional orthogonal multiple access (OMA), which has been considered as a key technology for 5G. NOMA in satellite communication system can provide anytime, anywhere access with improved spectral efficiency and system capacity because of its ubiquitous coverage. However, the characteristics of the satellite channels are different from that of the terrestrial network, i.e., huge time delay and Doppler shift. In this paper, different from the existing works, which mainly focus on the performance of NOMA in static terrestrial base stations and Geostationary orbit (GEO) scenarios, we investigate the performance analysis of downlink NOMA in dynamic low earth orbit (LEO) satellite communication system with Doppler shift considered. We combine NOMA and orthogonal frequency division multiplexing (OFDM) for better spectral efficiency. Our channel model includes both small scale model and large scale model. For simplify, we only consider two users in one spot beam. Besides, we express the performance analysis of downlink NOMA in LEO satellite communication system, like ergodic capacity, outage probability (OP) and mutual information. However, in traditional NOMA scheme, the proceeding error decision of the high power user will cause the deterioration of the subsequent detection performance. Therefore, a symmetrical coding (SC) scheme for different modulation mode is proposed for low power users to get better performance. Finally, simulation results validate the performance of the NOMA scheme is better than that of the OMA scheme. The proposed SC scheme can achieve a prominent increase performance contrasted to the traditional NOMA scheme.

**INDEX TERMS** LEO satellite communication system, NOMA, ergodic capacity, outage probability, mutual information, symmetrical coding scheme.

## I. INTRODUCTION

With the development of the wireless communication, the multiple access (MA) scheme has been the key technology to distinguish different wireless systems from the first generation (1G) to 4G [1]. These schemes divide time, frequency or code domain to different users to mitigate interference. However, these MA schemes cannot support the explosive data traffic and massive connectivity for the next generation wireless communication, i.e., 5G. NOMA has been proposed to address this problem [2]. Unlike OMA, by introducing some interference, multiple NOMA users' signals are multiplexed together by using different power allocation coefficients or different signatures such as

codebooks/codewords, sequences, interweavers, preambles, and the receiver decodes them in an successive interference cancellation (SIC) manner, which quite improved spectral efficiency. In this paper, we only focus on power-domain NOMA, so NOMA is referred as power-domain NOMA. Furthermore, the combination of LEO constellation and terrestrial network is the direction in 5G and the future wireless communication networks [3]–[6]. In [3], the authors establish a software-defined network (SDN) framework in the hybrid satellite-terrestrial networks for spectrum sharing, and propose second-priced auction to get optimal system performance. The authors of [4] present an architectural framework based on a layered approach comprising network, data link, and physical layers together with a multimode user terminal. The authors of [5] give a comprehensive review of recent research works concerning space-air-ground integrated

The associate editor coordinating the review of this manuscript and approving it for publication was Haipeng Yao<sup>1</sup>.

network from network design and resource allocation to performance analysis and optimization. Furthermore, [5] discusses several existing network architectures and points out some technology challenges and future directions.

In the previous literatures, some performance of NOMA has been investigated. In [6], a novel scheduling scheme is proposed to achieve full diversity and scheduling fairness, simultaneously. The simulation results show that the performance of the proposed NOMA scheme is superior to that of the OMA scheme. A closed-form expression of OP for the users in adaptive OMA/cooperative NOMA scheme is derived in [8], all users can achieve the same diversity. The outage performance of NOMA-based integrated satellite-terrestrial scenarios is investigated in [9] to [12]. The channel model is considered as small scale model, i.e., shadowed-Rician fading distribution, or large scale model, i.e., path loss, various atmospheric fading and rain induced attenuation. The simulation results verify the closed-form expression for OP. An iterative algorithm is proposed in [12] to get better outage performance.

There will be more than 1000-fold data traffic increase for 5G [1], so improving channel capacity is a significant aspect for future communication. We can find that the NOMA scheme can achieve superior performance in terms of ergodic sum rate than that of the OMA [7], [13]–[15]. In [7], a system-level performance of the NOMA scheme, for further LTE enhancement and future radio access, is studied. When considering channel estimation error, an optimal algorithm has been proposed in [13]. This algorithm maximizes sum rate in a more practical NOMA system. In [14], the authors propose a suboptimal power allocation scheme for NOMA in the cooperative relaying system to improve the spectral efficiency. A jointly optimization scheme of nodes power, UAVs heights and subchannel assignment for system capacity maximization in Multi-UAV scenario is investigated in [15].

From [16] to [18], the bit error rate performance (BER) of the NOMA system has been studied in fading channels, i.e., Rayleigh or Nakagami- $m$  fading channels. The BER performance of two users' and three users' system are presented in Nakagami- $m$  fading channels in [16]. By power allocation, it achieves fairness and minimizes average BER. Unlike the scheme in [16], in [17], the near user (NU), which has better channel condition, acts as a decode forward (DF) relay for the far user (FU). The NU sends the regenerated symbols of the FU to the FU. So the FU gets better performance than that of in [16]. As we all know, OFDM has already been used in 4G and will be used in 5G, OFDM based on Fast Fourier Transform (FFT) is used for conventional NOMA. A Discrete Wavelet Transform based pulse shaping technique for NOMA (WNOMA) has been proposed in [19]. The BER has been compared between the FFT-NOMA and WNOMA, theoretical and simulation BER results show that WNOMA outperforms FFT-NOMA in additive white Gaussian noise. By jointly searching for optimal subcarrier assignments of each user and power allocations over subcarriers,

minimization of the total transmit power under quality of service (QoS) has been achieved in [20].

However, in traditional SIC, the proceeding error decision of the high power user will cause the deterioration of the subsequent detection performance. To solve this problem, a symmetric superposition coding (SSC) and symmetric SIC (SSIC) decoding scheme are proposed to overcome the error propagation (EP) problem for downlink NOMA-based VLC network [21]. Based on [21], a bandwidth compression-symmetrical coding NOMA (BC-SCNOMA) system is proposed in [22], which benefits the BER performance of low power users. But the modulation mode of the users is the same in [21], [22]. It is not practical in many scenarios. Because different users with different QoS request may use different modulation mode. In this paper, thus, we propose a SC scheme for different modulation mode for downlink NOMA in LEO communication system.

References [6] to [8] and [13] to [21] above are studied in terrestrial scenarios, where the base stations (BS) and networks are easy to employ. There are still many places that BS cannot fit, i.e., ocean, desert and so on. However, satellite can provide ubiquitous coverage for users that cannot be served by BS. NOMA in satellite communication system can provide anytime, anywhere access with improved spectral efficiency and system capacity [23]–[30]. The concepts, techniques and challenges of Multi-satellite relay transmission (MSRT) in 5G are discussed in [23]. Two system models (TDMA and NOMA based MSRT) performance evaluation and three time scheduling strategies are introduced in [23]. In [24], a novel channel estimation algorithm is devised in multi-beam satellite NOMA system. In [25], it introduces a general overview of the application of the NOMA to various satellite architectures, for the benefits of meeting the requirements of 5G. Moreover, a NOMA scheme in downlink land mobile satellite network and a comprehensive performance analysis of the considered system are studied in [26]. In [27], [28], the combination of terrestrial network and satellite for NOMA is investigated. In [28], a new beamforming and power allocation algorithm is proposed, which is better than the algorithm in [27], the simulation results show that the sum rate in [28] is better than that of in [27]. The authors of [29] propose a novel QoS-guarantee resource allocation scheme for NOMA in satellite internet of things, achieving higher transmission performance. In [30], the OP performance of NOMA based cooperative spectrum sharing in hybrid satellite-terrestrial networks (HSTNs) is investigated. NOMA and spectrum sharing are used in terrestrial network. Although there are many literatures for NOMA studied related to satellite, the scenarios are almost in high earth orbit, i.e., GEO. The propagation delay is about 270ms from the terrestrial users to GEO satellite, which cannot meet the requirements of 5G. LEO satellite constellation has been a hot topic for many years, the combination of LEO satellite constellation and terrestrial network is the direction in 5G and the future wireless communication networks. In this paper, we will study the performance analysis of downlink NOMA

in LEO scenario with Doppler shift considered. We combine the NOMA and OFDM for better spectral efficiency. As we know, OFDM is sensitive to Doppler shift, the carrier frequency offset (CFO) will lead to inter-carrier interference. But NOMA is insensitive to CFO, because multiple users use the same resource block for transmission, which break the spectrum bottleneck of wireless communications [38], [39]. Ergodic capacity, OP, mutual Information and BER of 2 users in one LEO downlink beam will be investigated. A SC scheme for different modulation mode is proposed, which will help the NU get better performance. The main contributions can be summarized as follows:

- We study the performance analysis of downlink NOMA in dynamic LEO satellite communication system with Doppler shift considered. To best our knowledge, the aforementioned NOMA performance analyses based on satellite scenario are studied in GEO satellite communication system, which are static networks. We further combine the NOMA and OFDM for better spectral efficiency.
- Differ from [9] to [12], which only consider small scale model or large scale model, our channel model includes both small scale model and large scale model, which consider the path loss, various atmospheric fading, rain induced attenuation and Rician fading together.
- Moreover, in order to overcome the influence of error propagation on the performance of low power users, we propose a SC scheme for different modulation mode for practical. The SC scheme benefits both the mutual information and BER performance. Simulation results verify that the proposed SC scheme could achieve improved performance.

The remainder of this paper is organized as follows. Section II describes the system model, the related channel coefficient and the Doppler shift. In Section III, the performance analysis of downlink NOMA in LEO communication system, i.e., ergodic capacity, OP, mutual information, and the proposed SC scheme are introduced. Then numerical results are presented and analyzed in Section IV. Finally, Section V concludes this paper.

## II. SYSTEM MODEL

As illustrated in Fig. 1, consider a LEO satellite downlink communication system comprised with two users denoted by the NU and the FU. One multibeam LEO satellite denoted S. For simplify, we consider two users are located in the same spot beam, and the NU is located in the center of spot beam with better channel quality, the FU is located in the edge of spot beam with worse channel quality. The LEO satellite transmits signals to users on the same frequency and time slots with different power. Satellite and users are equipped with single antenna. Consider the geometry of the LEO orbit in Fig. 2. The LEO satellite orbit is circuit. Let  $i$  and  $h$  denote the inclination angle and the altitude of the orbit, respectively. Let  $\theta$  denotes the elevation angle of the user's

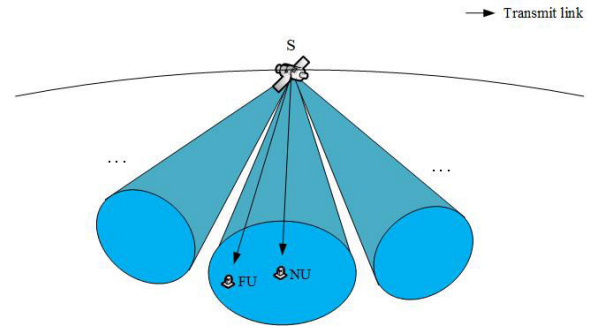


FIGURE 1. System model.

antenna. For the sake of math expression, we donate the NU and the FU as user 1 and user 2, respectively. By using NOMA scheme, user 1 and user 2 signals are transmitted together with different power. The transmitted signal at LEO satellite is expressed as

$$x = \sqrt{P_1}x_1 + \sqrt{P_2}x_2 \quad (1)$$

where  $P_1 = a_1P_s$  and  $P_2 = a_2P_s$  denote the transmit power allocated to user 1 and user 2, with the constrain  $a_1 + a_2 = 1$ .  $P_s$  is the transmit power of LEO satellite and  $a_1, a_2$  is the power allocation factor of user 1 and user 2, respectively.  $x_1, x_2$  are modulated symbols of users, i.e.,  $E[x_k^2] = 1, k = 1, 2$ .

By considering channel fading and Doppler shift, the received signal at user  $k, k = 1, 2$  is

$$y_k(t) = g_k(t) \cdot x \cdot e^{j2\pi f_d(t)t} + n_k(t) \quad (2)$$

where  $g_k(t)$  is the channel coefficient between the LEO satellite and user  $k, k = 1, 2$ .  $f_d(t)$  is the Doppler shift and  $t$  is the transmission time.  $n_k(t)$  denotes the additive white Gaussian noise (AWGN).

### A. CHANNEL COEFFICIENT

In this section, we will introduce the channel coefficient. According to simplified channel coefficient generation issued from [31], our scenario is a LEO satellite downlink with two users located in the same spot beam. Differ from the aforementioned papers [9]–[12], our channel model includes both the small scale model and the large scale model. The large scale model described as Section 6.6 of [32], the total path loss in dB ( $PL_{dB_k}$ ) of user  $k, (k = 1, 2)$  can be composed as Section 6.6.2 of [32]

$$PL_{dB_k} = PL_{bk} + PL_{gk} + PL_{sk} + PL_{ek} \quad (3)$$

where  $PL_{bk}, PL_{gk}, PL_{sk}$  and  $PL_{ek}$  are the basic path loss, the attenuation due to atmospheric gasses, the attenuation due to either ionosphere or tropospheric scintillation and the building entry loss in dB, respectively. The basic path loss in dB unit is modeled as [32]

$$PL_{bk} = FSPL_k + SF_k + CL_k \quad (4)$$

where  $FSPL_k$  is the free space path loss, the  $FSPL_k$  can be calculated as  $FSPL_k = 90.45 + 20 \lg(f_c) + 20 \lg(d_k(t))$  ( $f_c$  is the frequency in GHz,  $d_k(t)$  is link distance in km from the

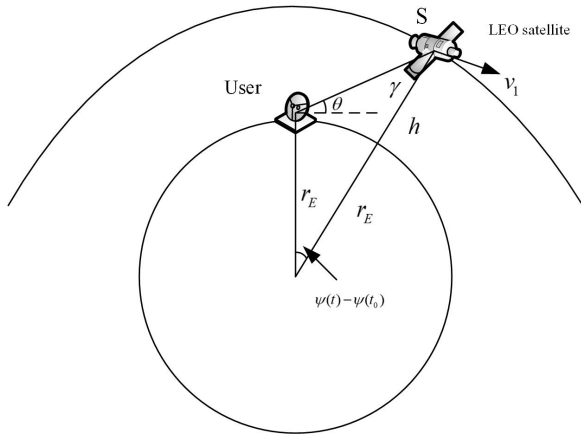


FIGURE 2. Geometry of the LEO orbit.

satellite to user  $k$ , ( $k = 1, 2$ ). As shown in Fig. 2, we can get  $d_k(t) = \sqrt{r_E^2 + (r_E + h)^2 - 2r_E(r_E + h) \cos(\psi(t) - \psi(t_0))}$ , where  $r_E$  is the radius of earth and  $\psi(t) - \psi(t_0)$  is the central angle presented as in Fig. 2.).  $CL_k$  is clutter loss [32], and  $SF_k$  is shadow fading loss, i.e.  $SF_k \sim N(0, \sigma_{SF_k}^2)$ . By assuming the losses in total path loss except shadow fading is fixed value and substituting (4) into (3), we can get that  $PL\_dB_k \sim N(u_{PL}, \sigma_{SF_k}^2)$ , the  $u_{PL}$  is the mean of the  $PL\_dB_k$  except  $SF_k$ . We assume that there is a line of sight for users to communicate via satellite and users are located in similar outdoor environment with experiencing nonselective fading due to diffuse multipath, which has constant power relative to the direct component [33], i.e., the small scale model is a Rician distribution, which can be expressed as  $a_k$ . After converting  $PL\_dB_k$  into general forms, i.e.,  $PL_k = 10^{\frac{PL\_dB_k}{10}}$ , the channel coefficient can be expressed as

$$g_k(t) = \sqrt{\frac{G_s G_u b_k(\varphi_k)}{PL_k}} a_k \quad (5)$$

where  $G_s$  and  $G_u$  are the antenna gain of the LEO satellite and the antenna gain of the users, respectively.  $b_k(\varphi_k)$  is the beam gain factor, it can be approximated as [34]

$$b_k(\varphi_k) = \left( \frac{J_1(u_k)}{2u_k} + 36 \frac{J_3(u_k)}{u_k^3} \right)^2 \quad (6)$$

with

$$u_k = 2.07123 \frac{\sin \varphi_k}{\sin \varphi_{3dB}} \quad (7)$$

where  $J(\cdot)$  is the Bessel function,  $\varphi_k$  is the angle between the location of the corresponding user and the beam center with respect to the LEO satellite, and  $\varphi_{3dB}$  is the 3-dB angle.

### B. DOPPLER SHIFT

In this section, we will consider the expression of Doppler shift, which can be composed as Equation (5) of [35]. We get (8), as shown at the bottom of the next page, where  $r = r_E + h$ ,  $\theta_{max}$  is the max elevation angle when the Doppler

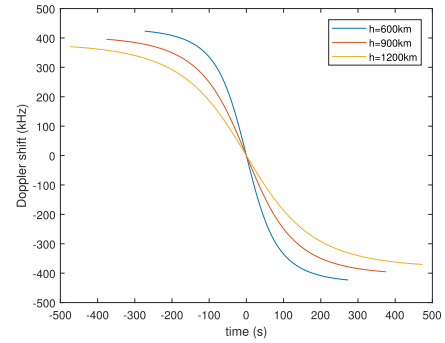


FIGURE 3. Doppler shift characterization curve.

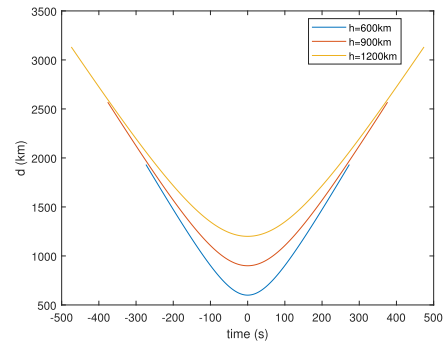


FIGURE 4. The distance between LEO satellite and users.

shift is minimum value and  $w_F(t)$  is the angular velocity of the LEO satellite in the orbit. For simplify, we set the inclination  $i = 0^\circ$ .  $t = 0$  when the max elevation angle  $\theta_{max} = 90^\circ$  and the users are located in the sub point. By considering the earth's autobiography, we assume that the LEO satellite rotates around the same direction as the earth, the  $w_F(t)$  can be expressed as

$$w_F(t) = w - w_0 \quad (9)$$

where  $w$  is the angular velocity of the LEO satellite and  $w_0$  is the angular velocity of the earth, i.e.,  $w = \sqrt{\frac{\mu}{(r_E + h)^3}}$ ,  $w_0 = 2\pi / (24 * 60 * 60)$  (rad/s),  $\mu$  is the Kepler constant, i.e.,  $\mu = 3.986 \times 10^{14} (m^3/s^2)$ . So  $\psi(t) - \psi(t_0)$  can be expressed as

$$\psi(t) - \psi(t_0) = (w - w_0)t \quad (10)$$

by substituting (9), (10) and other parameter into (8), the Doppler shift becomes

$$f_d(t) = -\frac{(w - w_0)}{c} \frac{r_E r \sin((w - w_0)t)}{\sqrt{r_E^2 + r^2 - 2r_E r \cos((w - w_0)t)}} \quad (11)$$

In visibility window, when we set the orbital altitude  $h = 600, 900$  and  $1200$  km, the Doppler shift characterization curve is presented in Fig. 3 and the distance between LEO satellite and users is presented in Fig. 4. From these figures, we can get that the visible time increases with the orbital altitude. The change rate of the Doppler shift and the distance between LEO satellite and users decrease as the orbital altitude  $h$  increases.

### III. PERFORMANCE ANALYSIS AND THE PROPOSED SC SCHEME

In this section, we will express performance analysis, i.e., ergodic capacity, OP and mutual information. A SC scheme for different modulation mode is proposed for user 1 to get better performance.

#### A. ERGODIC CAPACITY

According to NOMA scheme, by assuming successful demodulation and no error propagation, user 2 treats user 1 signal as noise and demodulates its own signal directly. So, the signal to noise plus interference ration (SNIR) of user 2 can be expressed as

$$SNIR_{2}(t) = \frac{a_2 SNR_t |H_2(t)|^2}{a_1 SNR_t |H_2(t)|^2 + 1} \quad (12)$$

By employing SIC, user 1 has to first demodulate  $x_2$  and subtract that component for the received signal  $y_1$ , and then to demodulate  $x_1$  without interference from  $x_2$ . The demodulating SNIR of user 1 to demodulate  $x_2$  is

$$SNIR_{2 \rightarrow 1}(t) = \frac{a_2 SNR_t |H_1(t)|^2}{a_1 SNR_t |H_1(t)|^2 + 1} \quad (13)$$

So the SNIR of user 1 can be expressed as

$$SNIR_1(t) = a_1 SNR_t |H_1(t)|^2 \quad (14)$$

where  $H_k(t) = g_k(t) * e^{j2\pi f_d(t) * t}$ , ( $k = 1, 2$ ),  $SNR_t = P_s / N_0$  is the transmission SNR. Thus, the sum rate of the two users can be written as

$$\begin{aligned} R_S(t) &= R_1(t) + R_2(t) \\ &= \log_2(1 + a_1 SNR_t |H_1(t)|^2) \\ &\quad + \log_2\left(1 + \frac{a_2 SNR_t |H_2(t)|^2}{a_1 SNR_t |H_2(t)|^2 + 1}\right) \end{aligned} \quad (15)$$

Farther more, the ergodic capacity can be expressed as

$$\begin{aligned} R_{erg}(t) &= \int_0^\infty R_1(t) f_{|H_1(t)|^2}(x) + R_2(t) f_{|H_2(t)|^2}(x) dx \\ &= \int_0^\infty \log_2(1 + a_1 SNR_t |H_1(t)|^2) f_{|H_1(t)|^2}(x) dx \\ &\quad + \int_0^\infty \log_2\left(1 + \frac{a_2 SNR_t |H_2(t)|^2}{a_1 SNR_t |H_2(t)|^2 + 1}\right) f_{|H_2(t)|^2}(x) dx \end{aligned} \quad (16)$$

where  $f_{|H_k(t)|^2}(x)$ , ( $k = 1, 2$ ) is the probability density function (PDF) of the  $|H_k(t)|^2$ , ( $k = 1, 2$ ).

#### B. OUTAGE PROBABILITY

The OP is defined as the probability that instantaneous SNIR falls below a predefined [26], which can be expressed as

$$\begin{aligned} P_{OP}(SNIR_{th}) &= P(SNIR_k(t) < SNIR_{th}) \\ &= F_{SNIR_k}(SNIR_{th}) \end{aligned} \quad (17)$$

where  $F_{SNIR_k}$  is the cumulative distribution function (CDF) of  $SNIR_k(t)$ , ( $k = 1, 2$ ).

#### C. MUTUAL INFORMATION

The mutual information is defined as a measure of the interdependence of variables, the user  $k$  ( $k = 1, 2$ ) mutual information between the transmitted signal and received signal can be expressed as

$$I(X; Y) = \sum_{y \in Y} \sum_{x \in X} p(x, y) \log\left(\frac{p(x, y)}{p(x)p(y)}\right) \quad (18)$$

where  $X, Y$  is the set of the transmitted signal and received signal,  $p(x, y)$  is the joint probability distribution function of  $x$  and  $y$ , while  $p(x)$  and  $p(y)$  are the marginal probability distribution functions of  $x$  and  $y$ , respectively.

#### D. THE PROPOSED SC SCHEME

In downlink NOMA, user 2 demodulates its data directly and user 1 with better channel condition needs to perform SIC to recover its signal. When user 1 demodulates user 2 signal incorrectly, extra interference will cause worse performance of user 1. So a SC scheme is proposed to solve this problem.

In this paper, BPSK modulation is employed for user 2. User 1 is used QPSK modulation. In Fig. 5, (a) is the traditional NOMA constellation and (b) is the constellation of the SC scheme for different modulation mode. The I axis is the decision boundary for user 2 signal symbols. The black dotted line and the R axis are the decision boundary for the first and the second bit of user 1 signal symbols. We can find that, compared with (a), when user 2 signal constellation points are on the left of the I axis, The real part of user 1 constellation points has changed signs, but user 2 has no change in (b), i.e., the constellation points of the low power users are symmetric about the decision boundary of the high power users. The main demodulation error of user 2 is that the constellation points near the I axis at the transmitter move to the other side of the coordinate axis when the points are demodulated. For example, the red point (01,1) moves to the area of the black point (11,0). This will cause demodulation error of user 1, i.e., the first bit 0 is demodulated as 1. In our proposed SC scheme, when the red point (01,1) moves to the area, which is the same as the traditional NOMA scheme, the user 1 signal symbol (01) is can still demodulated as (01),

$$f_d(t) = -\frac{w_F(t)}{c} \frac{r_E r \sin(\psi(t) - \psi(t_0)) \cos(\cos^{-1}(\frac{r_E}{r} \cos \theta_{max}) - \theta_{max})}{\sqrt{r_E^2 + r^2 - 2r_E r \cos(\psi(t) - \psi(t_0)) \cos(\cos^{-1}(\frac{r_E}{r} \cos \theta_{max}) - \theta_{max})}} \quad (8)$$

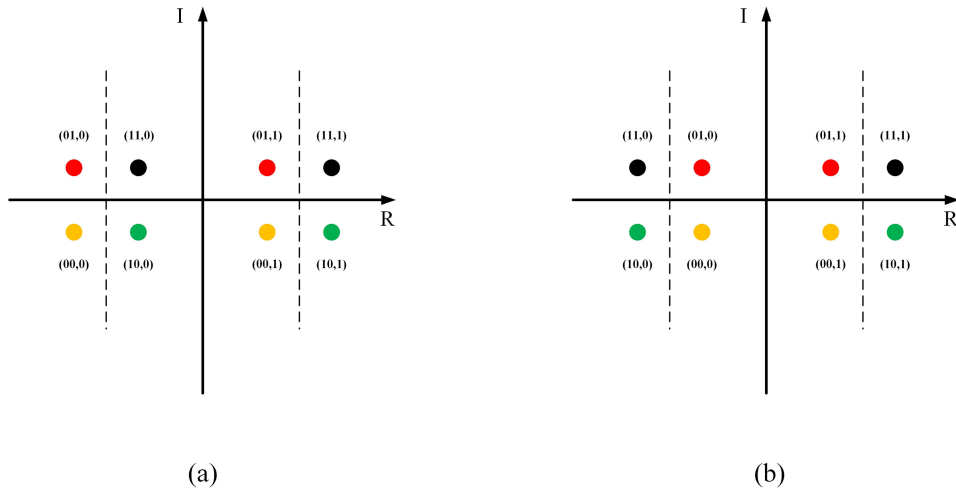


FIGURE 5. (a) The traditional NOMA constellation and (b) the constellation of the proposed SC scheme for different modulation mode.

**Algorithm 1** The Proposed SC Scheme

```

In transmitter:
if  $x_2 < 0$  then
     $x_1 = ((-1) * \text{real}(x_1) + j * \text{imga}(x_1))$ 
end if
 $x = \sqrt{a_2 P_s} x_2 + \sqrt{a_1 P_s} x_1$ 

In receiver:
User 2:
Demodulate  $y_2$  directly,  $\text{msg}_2 = \text{bpskdemod}(y_2)$ 

User 1:
Demodulate user 2 signal symbols firstly,  $\text{msg}_{2 \rightarrow 1} = \text{bpskdemod}(y_1)$ ;
Secondly, subtract user 2 signal symbols signal from the received signal  $y_1$ ,  $S_1 = y_1 - \text{bpskmod}(\text{msg}_{2 \rightarrow 1})$ ;
if  $\text{msg}_{2 \rightarrow 1} < 0$  then
     $S_1 = ((-1) * \text{real}(S_1) + j * \text{imga}(S_1))$ 
end if;
Finally, demodulate user 1 signal symbols,  $\text{msg}_1 = \text{qpskdemod}(S_1)$ 
    
```

although, the user 2 signal symbol is demodulated incorrectly. The SC scheme is summarized in **Algorithm 1**.

**IV. NUMERICAL RESULTS**

In this section, simulation results are provided to evaluate the performance analysis of downlink NOMA in LEO satellite communication system. Some parameters used in LEO satellite link are summarized in TABLE 1 [36], [37]. We set  $\varphi_1 = 0.1^\circ$ ,  $\varphi_2 = 0.3^\circ$ ,  $\varphi_{3dB} = 0.4^\circ$ ,  $PL_{gk} = 0$ ,  $PL_{sk} = 0$ ,  $PL_{ek} = 0$ ,  $\sigma_{SF_k} = 4$  dB, the Rician factor  $K_1 = 40$  dB,  $K_2 = 20$  dB. We assume the minimum elevation angle is 10 degrees and the time is 0 when Doppler shift is 0, i.e.,  $f_d(0) = 0$ .

**TABLE 1.** Parameters used in downlink NOMA system.

Parameter	Value
Carrier frequency	20GHz
Subcarrier spacing	120kHz
System bandwidth	480MHz
Number of FFT	512
User G/T ratio	2.6dB/K
User noise temperature	321K
Boltzmann constant	-228.68dBW/K/Hz
Satellite antenna gain	24.3dBi

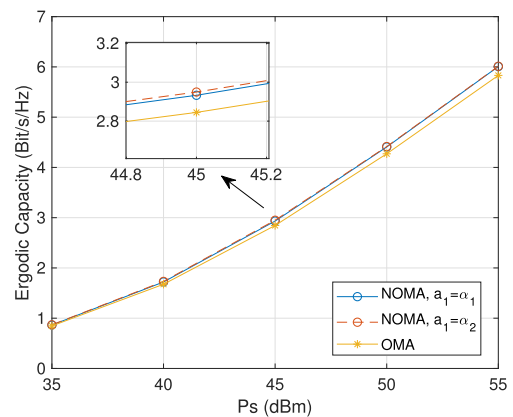


FIGURE 6. Ergodic capacity against transmit power in visibility window.

The comparison of average ergodic capacity for different transmit power between the NOMA and the OMA schemes in visibility window is plotted in Fig. 6. In order to assure that the sum rate of the NOMA scheme always outperforms that of the OMA scheme, the range of  $a_1$  can be expressed as

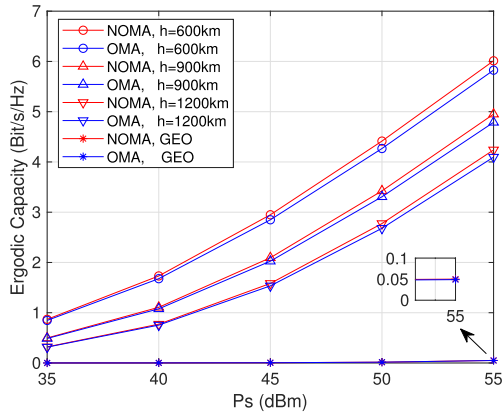


FIGURE 7. Ergodic capacity against transmit power with orbital altitude  $h$  in visibility window,  $\alpha_1 = \alpha_2$ .

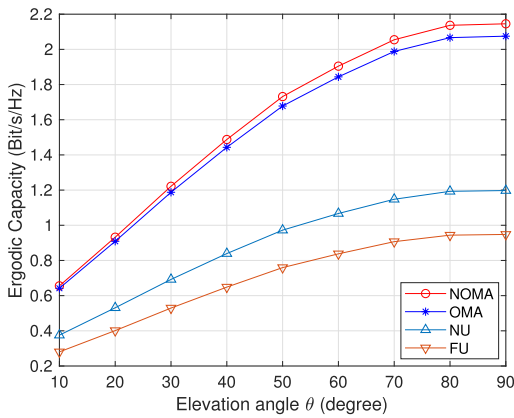


FIGURE 8. Ergodic capacity against elevation angle  $\theta$  in visibility window,  $P_s = 45$  dBm.

$\alpha_1 \leq a_1 \leq \alpha_2$  [26], where  $\alpha_1 = \frac{1}{\sqrt{1+SNR_t|H_1(t)|^2+1}}$ ,  $\alpha_2 = \frac{1}{\sqrt{1+SNR_t|H_2(t)|^2+1}}$ . We set  $a_1 = \alpha_1$ ,  $a_1 = \alpha_2$ , respectively. And we compare these NOMA schemes with OMA scheme. From the figure, the NOMA schemes are always superior to the OMA scheme. Furthermore, the maximization of average ergodic capacity is obtained when  $a_1 = \alpha_2$ .

Fig. 7 shows the average ergodic capacity of the NOMA and the OMA schemes against transmit power with orbital altitude  $h$ , when  $a_1 = \alpha_2$ . We find that when the orbital altitude  $h$  increases, the average ergodic capacity decreases, but the NOMA schemes are still superior to the OMA schemes. This is because that, on the one hand, when  $h$  increases, the path loss becomes quite larger than before, on the other hand, the NOMA schemes can use all time and frequency resources, while the OMA schemes only can use limited resources. Furthermore, when compared with NOMA in GEO satellite scenario [26] with same parameters, the ergodic capacity of NOMA in GEO satellite scenario is near to zero. NOMA in LEO communication system is much superior to NOMA in GEO satellite scenario. In order to achieve the same performance as the NOMA schemes in LEO communication system, the GEO satellite needs larger transmit power and receivers require larger gain. Fig. 8 presents the ergodic

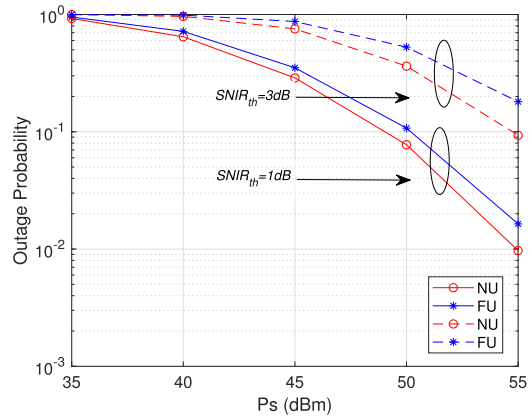


FIGURE 9. Outage probability against transmit power in visibility window.

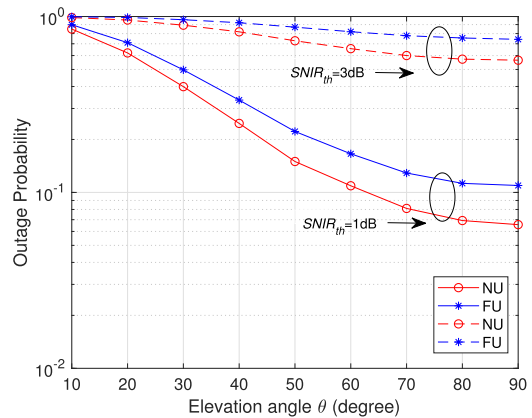


FIGURE 10. Outage probability against elevation angle  $\theta$  in visibility window,  $P_s = 45$  dBm.

capacity against elevation angle  $\theta$  in visibility window, when  $P_s = 45$  dBm. We find that, with the increasing of the elevation angle  $\theta$ , the performance of the NOMA scheme outperforms the OMA scheme. Although, the NU gets less transmit power than the FU, the ergodic capacity of the NU is still higher than that of the FU, as for the FU suffers worse channel condition. Hereinafter, we set the orbital altitude  $h = 600$  km and  $a_1 = \alpha_2$ .

The OP performance of the FU and the NU against transmit power and elevation angle  $\theta$  is illustrated in Fig. 9 and Fig. 10, respectively. We set the threshold  $SNIR_{th} = 1$  dB and  $SNIR_{th} = 3$  dB. Because the FU is in the edge of the beam and the channel quality is much worse than the NU, so the OP of the FU is quite bigger than the NU. When increasing the threshold from 1 to 3 dB, the OP performance of the FU and the NU degrades significantly. What is more, in Fig. 9, we set the transmit power is 45dBm. When the elevation angle  $\theta$  increases from 10 to 90 degrees in visibility window, the OP of two users also increases. The reason is that the Doppler shift and the distance between users and LEO satellite are becoming larger with the elevation angle  $\theta$  increasing, causing the channel coefficient decreasing and worse SNIR.

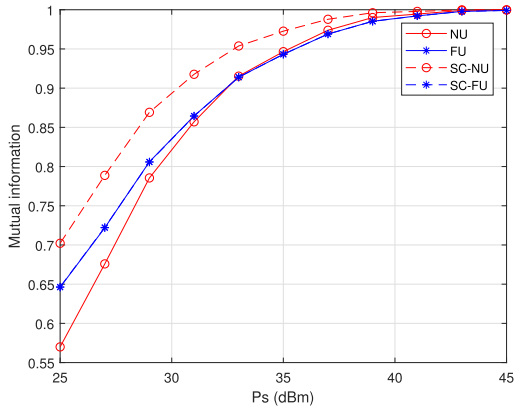


FIGURE 11. Mutual information against transmit power in visibility window.

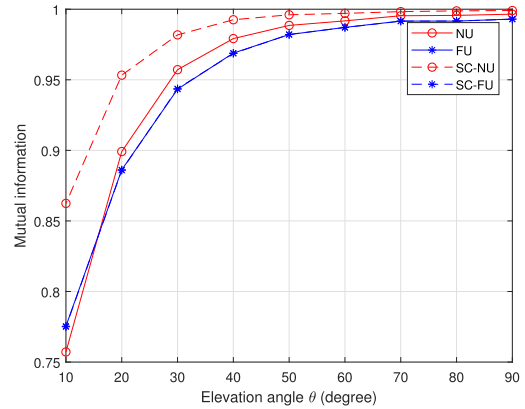


FIGURE 13. Mutual information against elevation angle  $\theta$  in visibility window,  $P_s = 35$  dBm.

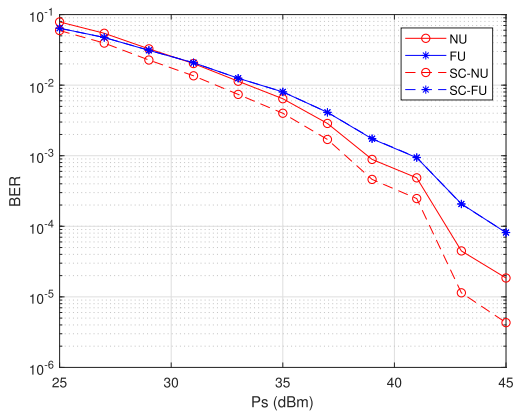


FIGURE 12. BER against transmit power in visibility window.

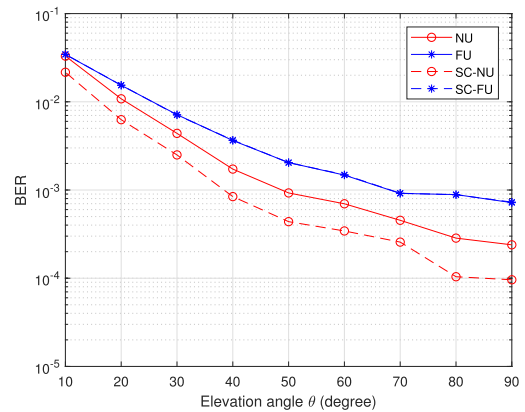


FIGURE 14. BER against elevation angle  $\theta$  in visibility window,  $P_s = 35$  dBm.

Fig. 11 and Fig. 12 present the average mutual information and average BER performance of the NU and the FU in visibility window, respectively. Similar to the OP and ergodic capacity, the BER performance of the NU is almost better than that of the FU. But for mutual information, when in low transmit power, the performance of the NU is inferior to that of the FU, when in high transmit power, the mutual information performance of the FU and the NU are almost consistent. The reason is that, when in lower transmit power, according to SIC scheme, the NU demodulates the FU signal incorrectly in a higher probability. This will cause extra interference to the NU signal with the loss of correlation to the NU transmit signal. However, when the transmission power is high, the SNR of the received signal in NU receiver is enough to demodulate the signal of the FU correctly. Through SIC, the NU can eliminate the interference of the FU from the received signal. So the mutual information performance of the FU and the NU is almost consistent in high transmit power.

The comparison of the average mutual information and average BER performance in the traditional NOMA and the proposed SC scheme are also shown in Fig. 11 and Fig. 12. Simulation results indicate that proposed SC scheme can achieve a prominent increase performance contrasted to the traditional NOMA scheme. The NU gets better mutual

information and BER performance in the proposed SC scheme. As depicted in Fig. 5, simulation results verify that, the proposed SC scheme has little effect on the performance of the FU with high transmit power. But for the NU in low power, because the proposed SC scheme eliminates some the effect of error propagation, gets higher mutual information and lower BER performance in the proposed SC scheme than that of the traditional NOMA scheme. Furthermore, the NU mutual information performance of the proposed SC scheme is superior to that of the FU.

The performance of mutual information against elevation angle  $\theta$  is conducted in Fig. 13. And BER performance against elevation angle  $\theta$  in visibility window is presented Fig. 14. When the elevation angle decreases from 90 to 10 degrees, the Doppler shift becomes larger. The huge Doppler shift deteriorates the channel coefficient. Thus, the BER and mutual information are worse when  $\theta$  decreases. Fig. 13 and Fig. 14 are also presented to verify the superiority of the proposed SC scheme against the tradition NOMA scheme. As indicated in Fig. 13, we compare the mutual information performance in the tradition NOMA scheme and the proposed SC scheme. The mutual information rises with the increasing of elevation angle  $\theta$ . The NU in the proposed SC scheme has better performance than that of traditional



NOMA scheme. As shown in Fig. 14, due to less Doppler shift, BER also gets better performance with the increasing of the elevation angle  $\theta$ . What's more, we can see that the BER performance of the NU in the proposed SC scheme has quite improved on the tradition NOMA scheme.

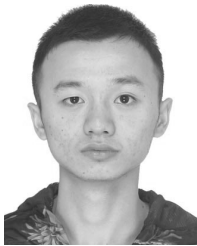
## V. CONCLUSION

In this paper, we first introduce a downlink NOMA scheme in LEO dynamic communication system. Secondly, we consider our model including both small scale model and large scale model and combine the NOMA and OFDM for better spectral efficiency. And then we give Doppler shift characterization curve, the distance between the LEO satellite and the users curve and the performance analysis. Besides, to overcome the extra interference caused by error propagation in the NU receiver, a SC scheme for different modulation mode is proposed, because different users with different QoS request may use different modulation mode. The simulation results demonstrated that the ergodic capacity of NOMA can be improved compared to that of OMA with transmit power or elevation angle  $\theta$  increasing. Furthermore, the OP and BER performance of the NU is better than that of the FU, although the NU is allocated less transmit power. By SIC, the NU signal improves reliability with the loss of correlation to the transmit NOMA signal, so the mutual information of the NU is not good as the FU. The simulation results also indicate that the proposed SC scheme has achieved better mutual information and BER performance than the traditional NOMA scheme for the NU.

## REFERENCES

- [1] L. Dai, B. Wang, Y. Yuan, S. Han, C.-L. I., and Z. Wang, "Non-orthogonal multiple access for 5G: Solutions, challenges, opportunities, and future research trends," *IEEE Commun. Mag.*, vol. 53, no. 9, pp. 74–81, Sep. 2015.
- [2] F. Boccardi, R. W. Heath, Jr., A. Lozano, T. L. Marzetta, and P. Popovski, "Five disruptive technology directions for 5G," *IEEE Commun. Mag.*, vol. 52, no. 2, pp. 74–80, Feb. 2014.
- [3] J. Du, C. Jiang, H. Zhang, Y. Ren, and M. Guizani, "Auction design and analysis for SDN-based traffic offloading in hybrid satellite-terrestrial networks," *IEEE J. Sel. Areas Commun.*, vol. 36, no. 10, pp. 2202–2217, Oct. 2018.
- [4] R. Gopal and N. BenAmmar, "Framework for unifying 5G and next generation satellite communications," *IEEE Netw.*, vol. 32, no. 5, pp. 16–24, Sep. 2018.
- [5] J. Liu, Y. Shi, Z. M. Fadlullah, and N. Kato, "Space-air-ground integrated network: A survey," *IEEE Commun. Surveys Tuts.*, vol. 20, no. 4, pp. 2714–2741, 4th Quart., 2018.
- [6] L. Yang, H. Jiang, Q. Ye, Z. Ding, L. Lv, and J. Chen, "On the impact of user scheduling on diversity and fairness in cooperative NOMA," *IEEE Trans. Veh. Technol.*, vol. 67, no. 11, pp. 11296–11301, Nov. 2018.
- [7] Y. Saito, A. Benjebbour, Y. Kishiyama, and T. Nakamura, "System-level performance evaluation of downlink non-orthogonal multiple access (NOMA)," in *Proc. IEEE 24th Annu. Int. Symp. Pers., Indoor, Mobile Radio Commun. (PIMRC)*, London, U.K., Sep. 2013, pp. 611–615.
- [8] K. Janghel and S. Prakriya, "Performance of adaptive OMA/cooperative-NOMA scheme with user selection," *IEEE Commun. Lett.*, vol. 22, no. 10, pp. 2092–2095, Oct. 2018.
- [9] X. Tang, K. An, K. Guo, Y. Huang, and S. Wang, "Outage analysis of non-orthogonal multiple access-based integrated satellite-terrestrial relay networks with hardware impairments," *IEEE Access*, vol. 7, pp. 141258–141267, 2019.
- [10] X. Yan, H. Xiao, C.-X. Wang, and K. An, "Outage performance of NOMA-based hybrid satellite-terrestrial relay networks," *IEEE Wireless Commun. Lett.*, vol. 7, no. 4, pp. 538–541, Aug. 2018.
- [11] S. Xie, B. Zhang, D. Guo, and W. Ma, "Outage performance of NOMA-based integrated satellite-terrestrial networks with imperfect CSI," *Electron. Lett.*, vol. 55, no. 14, pp. 793–795, Jul. 2019.
- [12] T. Qi, W. Feng, and Y. Wang, "Outage performance of non-orthogonal multiple access based unmanned aerial vehicles satellite networks," *China Commun.*, vol. 15, no. 5, pp. 1–8, May 2018.
- [13] J.-B. Kim and I.-H. Lee, "Capacity analysis of cooperative relaying systems using non-orthogonal multiple access," *IEEE Commun. Lett.*, vol. 19, no. 11, pp. 1949–1952, Nov. 2015.
- [14] Z. Ding, Z. Yang, P. Fan, and H. V. Poor, "On the performance of non-orthogonal multiple access in 5G systems with randomly deployed users," *IEEE Signal Process. Lett.*, vol. 21, no. 12, pp. 1501–1505, Dec. 2014.
- [15] R. Duan, J. Wang, C. Jiang, H. Yao, Y. Ren, and Y. Qian, "Resource allocation for multi-UAV aided IoT NOMA uplink transmission systems," *IEEE Internet Things J.*, vol. 6, no. 4, pp. 7025–7037, Aug. 2019.
- [16] T. Assaf, A. Al-Dweik, M. E. Moursi, and H. Zeineldin, "Exact BER performance analysis for downlink NOMA systems over Nakagami- $m$  fading channels," *IEEE Access*, vol. 7, pp. 134539–134555, 2019.
- [17] F. Kara and H. Kaya, "BER performances of downlink and uplink NOMA in the presence of SIC errors over fading channels," *IET Commun.*, vol. 12, no. 15, pp. 1834–1844, Sep. 2018.
- [18] F. Kara and H. Kaya, "On the error performance of cooperative-NOMA with statistical CSIT," *IEEE Commun. Lett.*, vol. 23, no. 1, pp. 128–131, Jan. 2019.
- [19] S. Baig, U. Ali, H. M. Asif, A. A. Khan, and S. Mumtaz, "Closed-form BER expression for Fourier and wavelet transform-based pulse-shaped data in downlink NOMA," *IEEE Commun. Lett.*, vol. 23, no. 4, pp. 592–595, Apr. 2019.
- [20] X. Li, C. Li, and Y. Jin, "Dynamic resource allocation for transmit power minimization in OFDM-based NOMA systems," *IEEE Commun. Lett.*, vol. 20, no. 12, pp. 2558–2561, Dec. 2016.
- [21] H. Li, Z. Huang, Y. Xiao, S. Zhan, and Y. Ji, "Solution for error propagation in a NOMA-based VLC network: Symmetric superposition coding," *Opt. Express*, vol. 25, no. 24, pp. 29856–29863, Nov. 2017.
- [22] M. Jia, Q. Gao, Q. Guo, X. Gu, and X. Shen, "Power multiplexing NOMA and bandwidth compression for satellite-terrestrial networks," *IEEE Trans. Veh. Technol.*, vol. 68, no. 11, pp. 11107–11117, Nov. 2019.
- [23] L. Bai, L. Zhu, X. Zhang, W. Zhang, and Q. Yu, "Multi-satellite relay transmission in 5G: Concepts, techniques, and challenges," *IEEE Netw.*, vol. 32, no. 5, pp. 38–44, Sep. 2018.
- [24] N. A. K. Beigi and M. R. Soleymani, "Interference management using cooperative NOMA in multi-beam satellite systems," in *Proc. IEEE Int. Conf. Commun. (ICC)*, Kansas City, MO, USA, May 2018, pp. 1–6.
- [25] X. Yan, K. An, T. Liang, G. Zheng, Z. Ding, S. Chatzinotas, and Y. Liu, "The application of power-domain non-orthogonal multiple access in satellite communication networks," *IEEE Access*, vol. 7, pp. 63531–63539, 2019.
- [26] X. Yan, H. Xiao, C.-X. Wang, K. An, A. T. Chronopoulos, and G. Zheng, "Performance analysis of NOMA-based land mobile satellite networks," *IEEE Access*, vol. 6, pp. 31327–31339, 2018.
- [27] X. Zhu, C. Jiang, L. Kuang, N. Ge, and J. Lu, "Non-orthogonal multiple access based integrated terrestrial-satellite networks," *IEEE J. Sel. Areas Commun.*, vol. 35, no. 10, pp. 2253–2267, Oct. 2017.
- [28] Z. Lin, M. Lin, J.-B. Wang, T. de Cola, and J. Wang, "Joint beamforming and power allocation for satellite-terrestrial integrated networks with non-orthogonal multiple access," *IEEE J. Sel. Topics Signal Process.*, vol. 13, no. 3, pp. 657–670, Jun. 2019.
- [29] X. Liu, X. Zhai, W. Lu, and C. Wu, "QoS-guarantee resource allocation for multibeam satellite industrial Internet of Things with NOMA," *IEEE Trans. Ind. Informat.*, early access, Nov. 6, 2019, doi: 10.1109/TII.2019.2951728.
- [30] X. Zhang, D. Guo, K. An, Z. Chen, B. Zhao, Y. Ni, and B. Zhang, "Performance analysis of NOMA-based cooperative spectrum sharing in hybrid satellite-terrestrial networks," *IEEE Access*, vol. 7, pp. 172321–172329, 2019.
- [31] S. Ahmadi, *New Radio Access Physical Layer Aspects, 5G NR*. S. Ahmadi, Ed. New York, NY, USA: Academic, 2019, pp. 285–409, Ch. 3, doi: 10.1016/B978-0-08-102267-2.00003-8.
- [32] *Propagation Data Required for the Design of Earth-Space Land Mobile Telecommunication Systems*, document Recommendation ITU-R, Dec. 2017.

- [33] F. Vatalaro, G. E. Corazza, C. Caini, and C. Ferrarelli, "Analysis of LEO, MEO, and GEO global mobile satellite systems in the presence of interference and fading," *IEEE J. Sel. Areas Commun.*, vol. 13, no. 2, pp. 291–300, Feb. 1995.
- [34] G. Zheng, S. Chatzinotas, and B. Ottersten, "Generic optimization of linear precoding in multibeam satellite systems," *IEEE Trans. Wireless Commun.*, vol. 11, no. 6, pp. 2308–2320, Jun. 2012.
- [35] I. Ali, N. Al-Dhahir, and J. E. Hershey, "Doppler characterization for LEO satellites," *IEEE Trans. Commun.*, vol. 46, no. 3, pp. 309–313, Mar. 1998.
- [36] W. Wang, Y. Tong, L. Li, A.-A. Lu, L. You, and X. Gao, "Near optimal timing and frequency offset estimation for 5G integrated LEO satellite communication system," *IEEE Access*, vol. 7, pp. 113298–113310, 2019.
- [37] A. Kalantari, G. Zheng, Z. Gao, Z. Han, and B. Ottersten, "Secrecy analysis on network coding in bidirectional multibeam satellite communications," *IEEE Trans. Inf. Forensics Security*, vol. 10, no. 9, pp. 1862–1874, Sep. 2015.
- [38] D. Zhang, Y. Liu, Z. Ding, Z. Zhou, A. Nallanathan, and T. Sato, "Performance analysis of non-regenerative Massive-MIMO-NOMA relay systems for 5G," *IEEE Trans. Commun.*, vol. 65, no. 11, pp. 4777–4790, Nov. 2017.
- [39] H. Zhang, N. Yang, K. Long, M. Pan, G. K. Karagiannidis, and V. C. M. Leung, "Secure communications in NOMA system: Subcarrier assignment and power allocation," *IEEE J. Sel. Areas Commun.*, vol. 36, no. 7, pp. 1441–1452, Jul. 2018.



**ZHIXIANG GAO** received the B.S. degree in communication engineering from the Army Engineering University of PLA, Nanjing, China, in 2018, where he is currently pursuing the M.S. degree with the College of Communication Engineering. His research interests include satellite communication and non-orthogonal multiple access (NOMA).



**AIJUN LIU** (Member, IEEE) received the B.S. degree in microwave communications and the M.S. and Ph.D. degrees in communications engineering and information systems from the College of Communications Engineering, Army Engineering University of PLA, Nanjing, China, in 1990, 1994, and 1997, respectively. He is currently a Full Professor with the Army Engineering University of PLA. His research interests include satellite communication system theory, signal processing, space heterogeneous networks, channel coding, and information theory.



**XIAOHU LIANG** received the B.S. degree in communication engineering from the University of Electronic Science and Technology of China (UESTC), Chengdu, China, in 2011, and the Ph.D. degree in information and communications engineering from the PLA University of Science and Technology (PLAUST), Nanjing, China, in 2016. He visited Lund University for researching the technique of faster-than-Nyquist signaling. He is currently a Faculty Member with the Army Engineering University of PLA. He also holds a postdoctoral position with the School of Information Science and Engineering, Southeast University (SEU), Nanjing. He hosted three projects, supported by the National Natural Science Foundation of China, the Natural Science Foundation of Jiangsu Province, and the China Postdoctoral Science Foundation. His research interests include non-orthogonal transmission technology and synchronization technique and massive MIMO.

...